



Article

# Malic Enzyme 1 Is Associated with Tumor Budding in Oral Squamous Cell Carcinomas

Chie Nakashima <sup>1,2</sup>, Tadaaki Kirita <sup>2,\*</sup> , Kazuhiko Yamamoto <sup>2</sup>, Shiori Mori <sup>1</sup>, Yi Luo <sup>3</sup>, Takamitsu Sasaki <sup>1</sup>, Kiyomu Fujii <sup>1</sup>, Hitoshi Ohmori <sup>1</sup>, Isao Kawahara <sup>1</sup>, Takuya Mori <sup>1</sup>, Kei Goto <sup>1</sup>, Shingo Kishi <sup>1</sup>, Rina Fujiwara-Tani <sup>1</sup> and Hiroki Kuniyasu <sup>1,\*</sup>

- <sup>1</sup> Department of Molecular Pathology, Nara Medical University, 840 Shijo-cho, Kashihara, Nara 634-8521, Japan; c-nakashima@naramed-u.ac.jp (C.N.); shi.m.0310@i.softbank.jp (S.M.); takamitsu@fc4.so-net.ne.jp (T.S.); toto1999-dreamtheater2006-sms@nifty.com (K.F.); brahmus73@hotmail.com (H.O.); isao\_kawahara@a011.broadband.jp (I.K.); pt\_mori\_t@yahoo.co.jp (T.M.); ilgfgtk@gmail.com (K.G.); nmu6429@yahoo.co.jp (S.K.); rina\_fuji@naramed-u.ac.jp (R.F.-T.)
- <sup>2</sup> Department of Oral and Maxillofacial Surgery, Nara Medical University, 840 Shijo-cho, Kashihara, Nara 634-8522, Japan; kazuyama@naramed-u.ac.jp
- <sup>3</sup> Key Laboratory of Neuroregeneration of Jiangsu and Ministry of Education, Co-Innovation Center of Neuroregeneration, Nantong University, Nantong 226001, China; lynantong@hotmail.com
- \* Correspondence: tkirita@naramed-u.ac.jp (T.K.); cooninh@zb4.so-net.ne.jp (H.K.); Tel.: +81-744-22-3051 (T.K. & H.K.); Fax: +81-744-25-7308 (H.K.)

Received: 27 August 2020; Accepted: 24 September 2020; Published: 28 September 2020



**Abstract:** Budding at the tumor invasive front has been correlated with the malignant properties of many cancers. Malic enzyme 1 (ME1) promotes the Warburg effect in cancer cells and induces epithelial–mesenchymal transition (EMT) in oral squamous cell carcinoma (OSCC). Therefore, we investigated the role of ME1 in tumor budding in OSCC. Tumor budding was measured in 96 human OSCCs by immunostaining for an epithelial marker (AE1/AE3), and its expression was compared with that of ME1. A significant correlation was observed between tumor budding and ME1 expression. The correlation increased with the progression of cancer. In human OSCC cells, lactate secretion decreased when lactate fermentation was suppressed by knockdown of ME1 and lactate dehydrogenase A or inhibition of pyruvate dehydrogenase (PDH) kinase. Furthermore, the extracellular pH increased, and the EMT phenotype was suppressed. In contrast, when oxidative phosphorylation was suppressed by PDH knockdown, lactate secretion increased, extracellular pH decreased, and the EMT phenotype was promoted. Induction of chemical hypoxia in OSCC cells by CoCl<sub>2</sub> treatment resulted in increased ME1 expression along with HIF1 $\alpha$  expression and promotion of the EMT phenotype. Hypoxic conditions also increased matrix metalloproteinases expression and decreased mitochondrial membrane potential, mitochondrial oxidative stress, and extracellular pH. Furthermore, the hypoxic treatment resulted in the activation of Yes-associated protein (YAP), which was abolished by ME1 knockdown. These findings suggest that cancer cells at the tumor front in hypoxic environments increase their lactate secretion by switching their energy metabolism from oxidative phosphorylation to glycolysis owing to ME1 overexpression, decrease in extracellular pH, and YAP activation. These alterations enhance EMT and the subsequent tumor budding. Tumor budding and ME1 expression are thus considered useful markers of OSCC malignancy, and ME1 is expected to be a relevant target for molecular therapy.

**Keywords:** ME1; tumor budding; EMT; extracellular pH; hypoxia

## 1. Introduction

Tumor budding refers to a small undifferentiated cancer cell cluster consisting of up to five cancer cells or a solitary cancer cell in the invasive front [1]. These cells are thought to acquire metastatic potential through the acquisition of an epithelial–mesenchymal transition (EMT) phenotype, characterized by decreased cell adhesion and enhancement of stemness [2]. Tumor budding has been shown to correlate with malignant properties in colorectal cancer and has been used as a prognostic marker [3,4]. In oral cancer, tumor budding correlates with lymph node metastasis and worse disease-free survival and overall survival and is considered a prognostic marker [5–7].

Hypoxia in advanced cancer microenvironment promotes tumor budding in colorectal cancer [8]. Genes whose expression is induced by hypoxia-inducible factor (HIF)-1 $\alpha$  activation by hypoxia promote EMT [9]. In addition, reprogramming of energy metabolism in a hypoxic environment, that is, suppression of oxidative phosphorylation and promotion of glycolysis and lactate fermentation, alter the properties of cancer [10]. In a previous study, we reported that overexpression of malic enzyme (ME)-1 in cancer promotes glutaminolysis, resulting in altered energy metabolism, from oxidative phosphorylation to glycolysis [11]. ME1 decarboxylates malic acid to form pyruvate and ultimately NADPH [12]. In cancer cells, pyruvate produced by ME1 is used for lactate fermentation [13,14]. ME1 expression in cancer cells also leads to energy metabolism reprogramming from oxidative phosphorylation to glycolysis, resulting in decreased oxygen consumption and increased lactate production, promoting tumorigenicity and tumor growth [11,15]. Taken together, the above findings suggest that ME1 might play an important role in tumor budding.

In this study, we investigated the role of ME1 in tumor budding in oral squamous cell carcinoma (OSCC), in which we had found a significant role for ME1 in tumor progression and EMT [11]. The results of this study are expected to clarify the mechanism of tumor budding and lead to the establishment of therapeutic strategies.

## 2. Results

### 2.1. Relationship between Tumor Budding and ME1 Expression in OSCC

To clarify the relationship between tumor budding and ME1 in OSCC, we performed immunostaining of the epithelial marker AE1/AE3 and of ME1 in 96 specimens of OSCC (Figure 1A and Table 1). As shown in Figure 1, ME1 expression was low in cases where budding was not seen at the tumor front, whereas it was higher in cases where budding was observed at the tumor front. As shown in Table 2, tumor budding and ME1 expression were significantly correlated with cancer progression according to both pT and pStage classifications. However, a significant correlation was observed only with ME1 with respect to grade and only with budding in the presence of lymph node metastasis.

Next, the correlation between the number of budding cells and ME1 expression was examined (Table 2). In all cases, a significant correlation was found between the two ( $p = 0.005$ ) (Figure 1B). Furthermore, when the correlation between tumor budding and ME1 expression was compared with T factor, N factor, and stage, a stronger correlation was observed in cases that progressed with respect to all factors. This suggests that tumor budding and ME1 are deeply involved in the progression of OSCC.

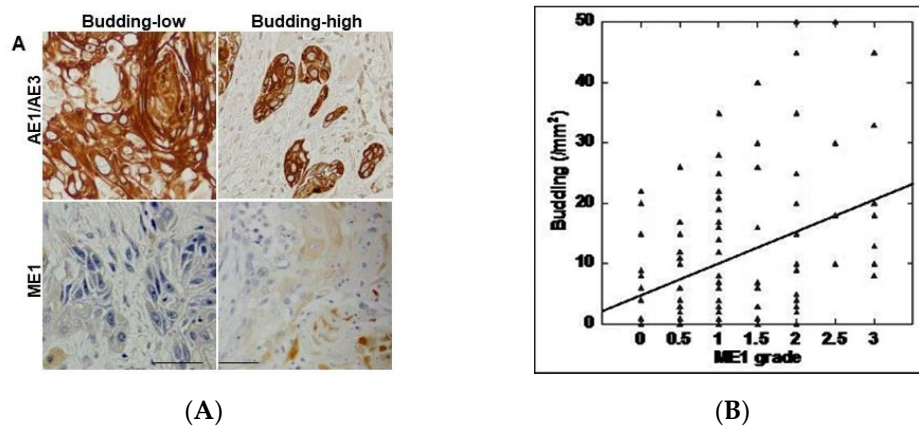


**Figure 1.** Relationship between tumor budding and malic enzyme 1 expression. (A) Tumor budding confirmed by AE1/AE3 immunostaining and ME1 immunoreactivity. Scale bar, 100  $\mu\text{m}$ . (B) Correlation between tumor budding and ME1 expression by Spearman regression model. Spearman  $r = 0.284$ ,  $p < 0.005$ . ME1, malic enzyme 1; AE1/AE3, cytokeratin AE1/AE3.

**Table 1.** Relationship between ME1 expression or tumor budding and clinicopathological parameters in 96 oral squamous cell carcinomas.

Parameter	Case Number	ME1 Expression	$p^*$	Budding ( $\mu\text{m}^2$ )	$p^*$
Age (years)					
$\leq 59$	59	$1.28 \pm 0.81$		$14.2 \pm 15.1$	
$\leq 60$	37	$1.12 \pm 0.89$	NS	$10.0 \pm 14.1$	NS
Sex					
F	14	$1.29 \pm 0.96$		$10.8 \pm 8.2$	
M	82	$1.21 \pm 0.083$	NS	$12.9 \pm 15.7$	NS
Site					
Gingiva	26	$1.19 \pm 0.71$		$15.6 \pm 17.5$	
Tongue	35	$1.41 \pm 0.94$		$13.1 \pm 10.0$	
Pharynx	17	$1.09 \pm 0.69$		$12.1 \pm 16.1$	
Floor	18	$1.56 \pm 1.00$	NS	$11.5 \pm 18.1$	NS
Grade					
1	38	$1.5 \pm 0.8$		$12.5 \pm 15.4$	
2	29	$1.3 \pm 0.9$		$13.8 \pm 16.4$	
3	29	$0.8 \pm 0.7$	0.0199	$11.6 \pm 12.3$	NS
pT					
1	13	$0.9 \pm 1.0$		$2.8 \pm 6.2$	
2	37	$1.3 \pm 0.8$		$5.1 \pm 4.4$	
3	39	$1.2 \pm 0.8$		$19.4 \pm 11.1$	
4	7	$2.1 \pm 0.3$	0.0175	$22.1 \pm 24.8$	<0.0001
pN					
0	57	$1.3 \pm 0.9$		$10.9 \pm 12.1$	
1	28	$1.1 \pm 0.7$		$14.9 \pm 13.9$	
2	11	$1.4 \pm 0.8$	NS	$18.8 \pm 11.5$	<0.0001
pStage					
1	7	$1.0 \pm 1.2$		$1.6 \pm 2.9$	
2	22	$1.4 \pm 0.9$		$3.7 \pm 4.4$	
3	60	$1.1 \pm 0.8$		$14.8 \pm 11.3$	
4	7	$2.1 \pm 0.3$	0.0156	$22.1 \pm 24.8$	<0.0001

Tumor progression, stage, and histological grades were determined according to the Union for International Cancer Control TNM classification system [16]. NS, not significant. \*  $p$  value is calculated by Student's  $t$ -test.

**Table 2.** Correlation between ME1 expression and tumor budding.

Parameters	Case Number	Spearman r	<i>p</i> *
All cases	96	0.284	0.005
pT1–2	50	0.3633	0.0103
pT3–4	46	0.4783	0.0004
pN0	57	0.3085	0.0132
pN1–2	39	0.5624	0.0016
pStage1–2	29	0.3023	0.0129
pStage3–4	67	0.5599	<0.0001

Tumor progression and stage were determined according to the Union for International Cancer Control TNM classification system [16]. \* *p* value is calculated by Spearman r regression test.

## 2.2. Effect of ME1 on Extracellular pH

The EMT phenotype has been identified as a malignant characteristic of budding cancer cells [2]. Our previous studies revealed that ME1 promotes the Warburg effect and is involved in the induction of EMT [11]. Therefore, we examined the relationship between the Warburg effect and EMT. First, ME1 was knocked down in the human oral SCC cell line HSC4, and the expression of EMT-related factors was examined (Figure 2A). Knockdown of ME1 increased the expression of E-cadherin and claudin (CLDN)-4 and decreased the expression of HIF-1 $\alpha$ . Furthermore, the possible alteration in extracellular pH was examined by considering the effect of ME1 on the Warburg effect (Figure 2B). Knockdown of ME1 altered the acidic extracellular pH to neutral. Lactate dehydrogenase A (LDHA) was then knocked down to confirm that the alteration in the extracellular pH was due to changes in glycolysis–lactate fermentation (Figure 2C,D). Consequently, lactate level in the culture solution decreased, and the pH increased. To investigate the effect of extracellular pH on EMT, the pH of the culture solution was adjusted to 7.6 and 6.8, and HSC4 cells were cultured (Figure 2E). In the acidic culture medium, E-cadherin expression was decreased, and vimentin expression was increased, which indicated that the EMT phenotype was induced in the acidic culture medium compared with the neutral culture medium.

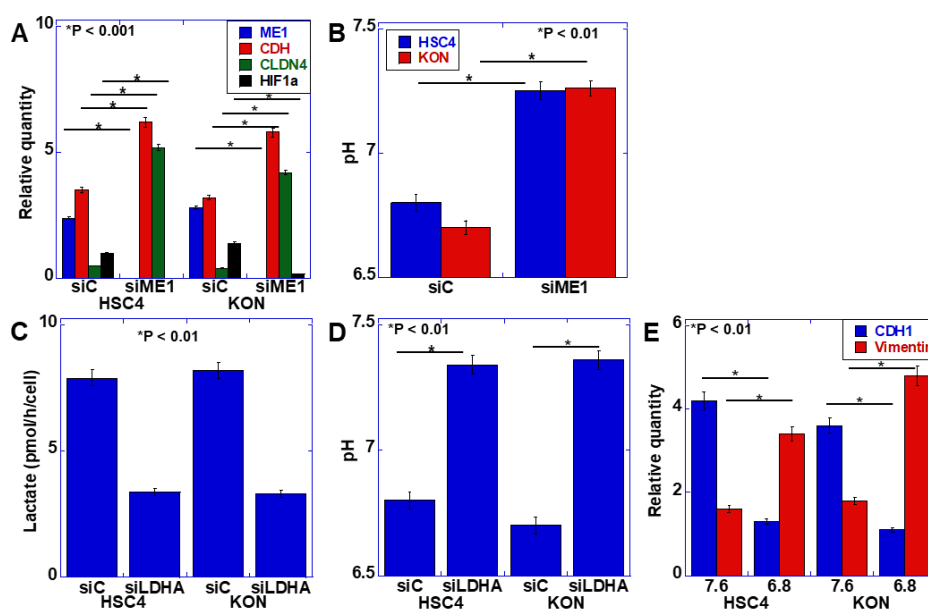


**Figure 2.** Effect of extracellular pH on the epithelial–mesenchymal transition (EMT) phenotype in HSC4 and KON oral squamous cell carcinoma (OSCC) cells. (A,B) Effect of the knockdown of ME1 on mRNA expression of EMT-associated genes measured by quantitative PCR (A) and extracellular pH

(B) in HSC4 and KON cells. (C,D) Effect of the knockdown of lactate dehydrogenase A (LDHA) on extracellular lactate concentration (C) and pH (D) in HSC4 and KON cells. (E) Effect of medium pH on the EMT phenotype in HSC4 and KON cells. Expression was measured by quantitative PCR. Error bar, standard deviation tested by Student's *t*-test in three independent trials. CDH, E-cadherin; CLDN, claudin; HIF, hypoxia-inducible factor; siRNA, small interference RNA; siME, siRNA for ME1; siC, control siRNA; siLDHA, siRNA for LDHA.

### 2.3. Relationship between the Warburg Effect and Lactate Secretion

EMT was induced by the acidification of the extracellular pH, suggesting that the transition promoted by ME1 from oxidative phosphorylation of energy production to glycolysis and lactate fermentation is important for EMT acquisition. Therefore, we next knocked down pyruvate dehydrogenase (PDH), which induces oxidative phosphorylation through metabolism of pyruvate, the final metabolite of glycolysis, or inhibited PDH kinase, which induces glycolysis by dichloroacetate (DCA) (Figure 3A–C). Knockdown of PDH increased lactate production and decreased the extracellular pH (Figure 3A). In contrast, inhibition of PDH kinase decreased lactate production and increased the extracellular pH (Figure 3B). On examining the expression of CLDN4 and HIF1 $\alpha$ , which are involved in the EMT phenotype (Figure 3C), CLDN4 expression was found to be decreased, and HIF1 $\alpha$  expression was enhanced by PDH knockdown, indicating promotion of the EMT phenotype. In contrast, inhibition of PDH kinase increased CLDN4 expression and decreased HIF1 $\alpha$  expression, indicating suppression of the EMT phenotype.

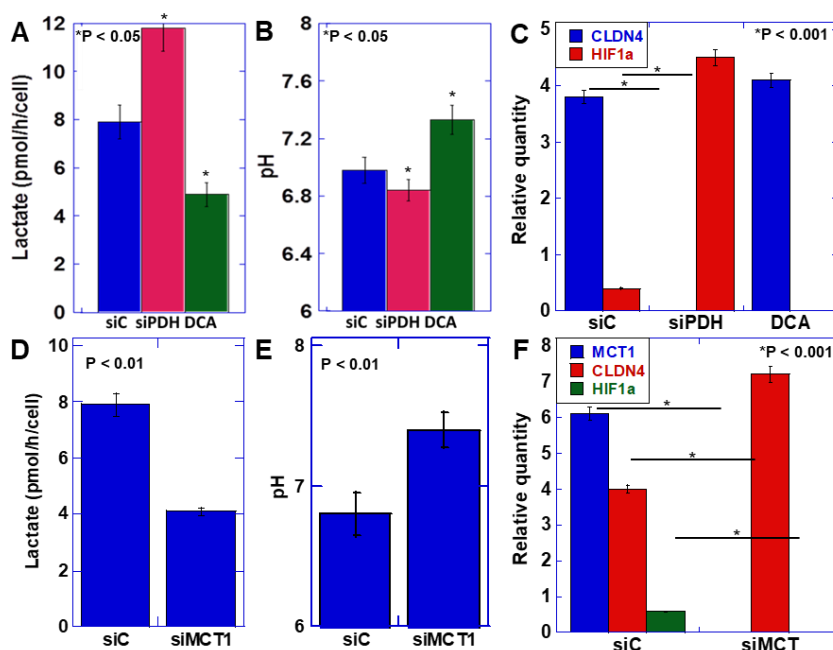


**Figure 3.** Effect of lactate on the EMT phenotype in HSC4 OSCC cells. (A–C) Effect of knockdown of pyruvate dehydrogenase (PDH) or inhibition of PDH kinase by dichloroacetate (DCA) on extracellular lactate (A), extracellular pH (B), and mRNA expression of EMT-associated genes measured by quantitative PCR (C) in HSC4 cells. (D–F) Effect of knockdown of monocarbonate transporter (MCT)1 on extracellular lactate (D), extracellular pH (E), and mRNA expression of EMT-associated genes measured by quantitative PCR (F) in HSC4 cells. Error bar, standard deviation tested by Student's *t*-test in three independent trials. siPDH, siRNA for PDH; siMCT1, siRNA for MCT1.

Next, to confirm the significance of lactate secretion compared with the increase in intracellular lactate levels, the monocarbonate transporter (MCT)-1, which promotes secretion of lactate extracellularly, was knocked down. (Figure 3D–F). As a consequence, the extracellular lactate

level was found to decrease, and the extracellular pH increased. At this time, CLDN4 expression increased, and HIF1 $\alpha$  expression decreased, indicating suppression of the EMT phenotype. As observed above, the decrease in extracellular pH due to the increase in lactate secretion accompanying the enhancement of the Warburg effect induced the EMT phenotype.

#### 2.4. Effects of Hypoxic Environment on Cancer Cells

We next examined the effect of hypoxic environment, which is characteristic of budding cancers, on cancer cells [17] (Figure 4). Cell proliferation was examined after treating both oral SCC cell lines with various concentrations of CoCl<sub>2</sub> to induce a chemical hypoxic environment (Figure 4A). In both cell lines, growth inhibition of 20–30% was observed at 100  $\mu$ M of CoCl<sub>2</sub>. In HSC4 and KON cells, treatment with 100  $\mu$ M CoCl<sub>2</sub> increased the expression of matrix metalloproteinase (MMP)9 and MMP7 but not of MMP2 (Figure 4B). CoCl<sub>2</sub> treatment increased the expression of ME1 and HIF1 $\alpha$  and decreased the expression of CLDN4 in HSC4 cells (Figure 4C). The expression of c-Myc, which promotes glycolysis, was also enhanced. In contrast, in the hypoxic environment, mitochondrial membrane potential, extracellular pH, and mitochondrial reactive oxygen species (ROS) levels were decreased in both cell lines (Figure 4D–F).

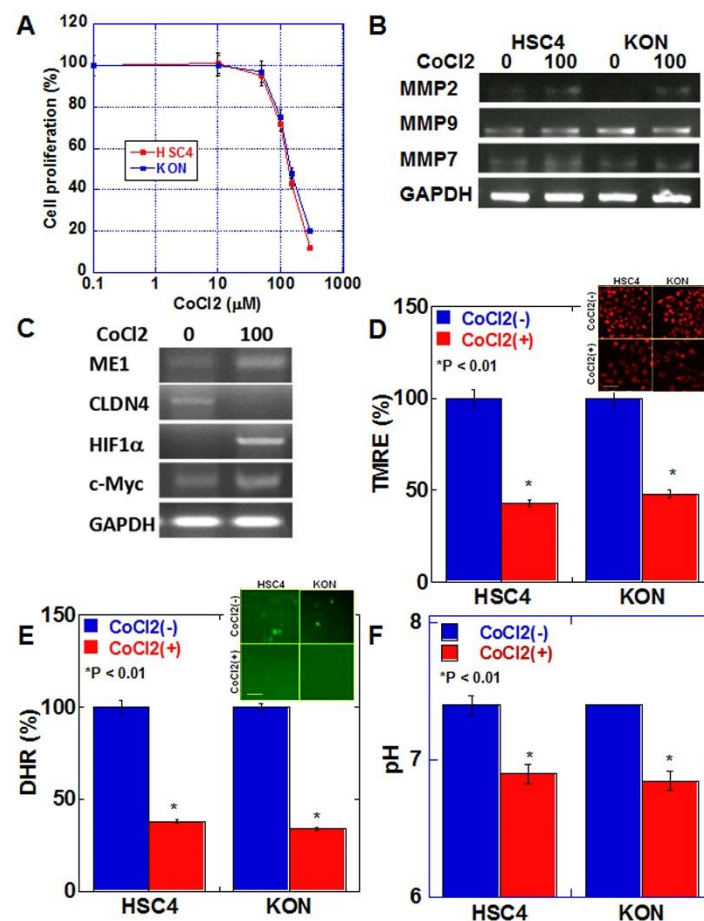


**Figure 4.** Effect of hypoxia on EMT and mitochondrial function in HSC4 and KON OSCC cells. (A) Effect of CoCl<sub>2</sub>-induced hypoxia on cell proliferation in HSC4 and KON OSCC cells. (B) Effect of hypoxia on mRNA expression of MMPs in HSC4 and KON OSCC cells. (C) Effect of hypoxia on mRNA expression of EMT-associated genes. (D–F) Effect of hypoxia on mitochondrial membrane potential (TMRE assay). (D), mitochondrial reactive oxygen species (ROS, DHR assay) (E), and extracellular



pH (F). Inserts in (D,E) show fluorescent images. Error bar, standard deviation tested by Student's *t*-test in three independent trials. Scale bar, 50  $\mu$ m. GAPDH, glyceraldehyde 3-phosphate dehydrogenase; TMRE, tetramethylrhodamine ethyl ester; ROS, reactive oxygen species; DHR123, dihydrorhodamine 123.

### 2.5. Yes-Associated Protein (YAP) Activation by ME1

In a previous study, we reported that YAP activation induces the EMT phenotype in oral SCC [18]. Therefore, YAP activation as the EMT induction mechanism by ME1 was examined by knocking down ME1 (Figure 5A,B). Knockdown of ME1 increased the phosphorylation levels of YAP and large tumor suppressor (LATS) and decreased nuclear YAP levels. This suggested that YAP is activated by ME1. In addition, hypoxic treatment increased nuclear YAP levels (Figure 5C).

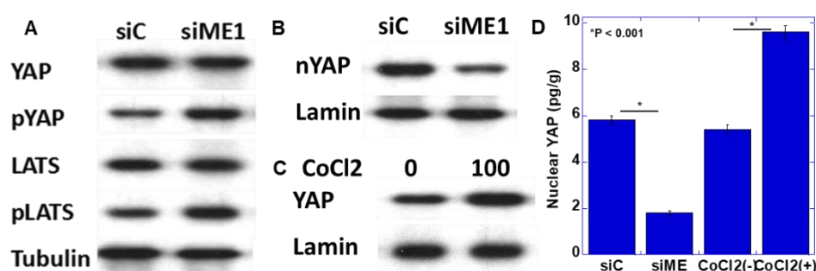


**Figure 5.** Effect of ME1 and hypoxia on yes-associated protein (YAP) activation in HSC4 OSCC cells. (A,B) Effect of knockdown of ME1 on phosphorylation (A) and nuclear translocation (B) of YAP in HSC4 cells. (C) Effect of CoCl<sub>2</sub>-induced hypoxia on nuclear translocation of YAP in HSC4 cells. (D) Concentrations of nuclear YAP were measured by ELISA. Tubulin and lamin were examined as loading controls. pYAP, phosphorylated YAP; LATS, large tumor suppressor; pLATS, phosphorylated LATS; siME, siRNA for ME1.

### 3. Discussion

In the present study, budding at the invasive front of cancer was found to be closely related to cancer progression. It has been suggested that a hypoxic environment, promotion of the Warburg effect, decrease in extracellular pH, and EMT are responsible for tumor budding and acquisition of the malignant phenotype. Furthermore, ME1 plays an important role in this process.

At the invasive front, cancer cells tend to experience hypoxia because they invade the stromal tissue with low blood vessel density. In oral melanoma, it has been reported that hypoxia is seen at the invasive front, and hypoxia responses such as HIF1 $\alpha$  and vascular endothelial growth factor (VEGF) upregulation have been observed [17]. Our study also showed that alterations in HIF1 $\alpha$  and ME1 expression occurred concomitantly, suggesting a relationship between tumor budding and hypoxia. Furthermore, it was revealed that the expression of ME1 was induced by hypoxia. A previous study reported that ME1 expression is lowered by HIF1 $\alpha$  knockdown [19]. These findings suggest that ME1 is an HIF1 $\alpha$  target gene, and ME1 overexpression at the invasive front can be considered as a hypoxic response.

In a hypoxic environment, expression of MMP9 and MMP7 is upregulated by HIF1 $\alpha$  activation [20,21]. Our data showed increase of MMP9 and MMP7 in hypoxic conditions, which suggests increase of invasion ability. VEGF, whose secretion is induced by hypoxia, promotes angiogenesis and lymphangiogenesis, facilitating the metastatic spread of cancer cells [22]. Hypoxia activates Jagged2 and promotes stemness and EMT via NOTCH and AKT signals [23]. Furthermore, hypoxic cancers are more invasive and have a poorer prognosis than non-hypoxic cancers [24]. Thus, hypoxia is deeply associated with the promotion of the tumor budding phenotype.

Since hypoxia is strongly involved in tumor budding, we examined the energy metabolism associated with the hypoxic environment and found that ME1 expression and lactate levels were

increased. Liao et al. reported that ME1 expression in cancer cells leads to energy metabolism reprogramming from oxidative phosphorylation to glycolysis, resulting in decreased oxygen consumption, increased lactate production, and subsequent promotion of tumorigenicity and tumor growth [11,15]. According to our data, hypoxia decreased the mitochondrial membrane potential, suppressed oxidative phosphorylation, and decreased oxidative stress. A correlation between budding at the invasive front and promotion of glycolysis via increased GLUT1 expression, which enhances glucose intake, has been previously reported [25]. Fructose-1,6-biophosphate promotes oxidative phosphorylation but is suppressed by EMT-inducing Snail, resulting in a switch in the glycolytic pathway of energy metabolism during the EMT process [26]. Thus, a mutual promotive relationship is suggested between energy metabolism reprogramming and EMT phenotype at the tumor invasive front.

Furthermore, in this study, lactate secretion increased and extracellular pH decreased as a result of promotion of the Warburg effect. The decrease in extracellular pH was strongly correlated with EMT. A decrease in extracellular pH promotes growth, migration, invasion, and metastasis of cancer cells in an acidic environment via GPR4, GPR65 (TDAG8), GPR68 (OGR1), and GPR132 (G2A), which are pH-sensing G protein-coupled receptors (GPCRs) [27].

An acidic extracellular pH also suppresses immune cells and reduces responsiveness to anti-cancer drugs [27]. We have also reported that impairment of the barrier function of tight junctions by an anti-CLDN4 antibody raises the pH of the tumor microenvironment and reduces the stemness of cancer cells [28]. In addition, a low pH in the cancer cell microenvironment promotes infiltration of myeloid-derived suppressor cells, regulatory T cells, and tumor-associated macrophages and induces PD-L1 expression in cancer cells, which impairs T-cell antitumor immunity [29]. Acidification of the cancer microenvironment is thought to be caused by increased lactate secretion. In our study, the inhibition of pyruvate metabolism to acetyl-CoA by PDH knockdown increased lactate production and decreased the extracellular pH. Conversely, LDHA knockdown and PDH activation by PDH kinase inhibition reduced lactate and increased the extracellular pH. Furthermore, the extracellular pH was increased by knocking down MCT1, which is a transporter that secretes lactate. Extracellular carbonic anhydrases and monocarboxylate transporters are also known to play an important role in inducing a low extracellular pH under hypoxia, which promotes invasion, metastasis, and stemness of cancer cells [29].

In our study, YAP was activated in a hypoxic environment and was abrogated by knockdown of ME1. We already showed that YAP activation is a significant factor that promotes the EMT phenotype and is deeply involved in the progression of oral SCC [18]. In hypoxia, YAP is activated through upregulation of GPRC5A by HIF1 $\alpha$  [30]. Reciprocally, activated YAP stabilizes HIF1 $\alpha$  and enhances its action [31]. In addition, YAP is activated by enhanced glycolysis–lactate fermentation [32]. The inhibition of YAP activation by ME1 knockdown observed in our study is considered to be associated with the suppression of ME1 energy metabolism reprogramming. Thus, YAP is thought to induce EMT in response to hypoxia and energy metabolism reprogramming.

As described above, reprogramming of the energy metabolism pathway from oxidative phosphorylation to glycolysis–lactate fermentation, increased lactate secretion, and consequent YAP activation were closely involved in the induction of the EMT phenotype. Furthermore, the extracellular pH increased due to ME1 knockdown, suggesting that ME1 is strongly involved in energy metabolism reprogramming.

## 4. Materials and Methods

### 4.1. Tissue Arrays

Tissue array slides of OSCCs (96 cases) were obtained from US Biomax Inc. (Rockville, MD, USA). Duplet slides were immunostained with anti-ME1 and anti-AE1/AE3 antibodies (Abnova Corporation, Taipei City, Taiwan), and the association between clinicopathological parameters and ME1 expression levels was determined.



#### 4.2. Immunohistochemistry

Formalin-fixed, paraffin-embedded surgical specimens were cut into 4  $\mu\text{m}$ -thick sections. Consecutive 4  $\mu\text{m}$  sections were immunohistochemically stained using the immunoperoxidase technique described previously [33]. The sections were incubated with 0.5  $\mu\text{g}/\text{mL}$  anti-ME1 or anti-AE1/AE3 antibodies for 2.5 h at room temperature. Secondary antibodies (Dako, Carpinteria, CA, USA) were applied for 1 h. Tissue sections were color-developed with diaminobenzidine hydrochloride (Dako) and counterstained with Meyer's hematoxylin (Sigma Chemical Co., St. Louis, MO, USA). ME1 immunoreactivity was classified according to our previous study [11]. Grade 0 indicates no expression, Grade 1 indicates an expression equivalent to that in normal oral squamous epithelium, Grade 2 is an intermediate expression, and Grade 3 indicates strong expression [34].

#### 4.3. Human OSCC Cell Lines

We purchased HSC4 and KON human OSCC cell lines from Dainihon Pharmaceutical Co. (Tokyo, Japan). Cells were cultured and maintained in Dulbecco's modified Eagle's medium (DMEM) supplemented with 10% fetal bovine serum (FBS) at 37 °C in 5%  $\text{CO}_2$ . Cell growth was assessed using the 3-(4,5-dimethylthiazol-2-yl)-5-(3-carboxymethoxyphenyl)-2-(4-sulfophenyl)-2H-tetrazolium (MTS) assay, as previously described [33]. Culture media with pH 7.6 and pH 6.9 were prepared by adjusting the pH with EDTA and HCl (WAKO), respectively, from regular DMEM.  $\text{CoCl}_2$  and DCA were purchased from WAKO Pharmaceutical Co. Ltd. (Osaka, Japan).

#### 4.4. Extracellular pH

Cells ( $1 \times 10^4$ ) were cultured with 2 mL of DMEM for 48 h. The pH of the culture medium was measured with a pH meter (Chemical Instruments, Co. Ltd., Hachioji, Japan).

#### 4.5. Small Interfering RNA

Stealth Select RNAi (siRNA) for human ME1, LDHA, PDH, and MCT1 was purchased from Santa Cruz Biotechnology. AllStars Negative Control siRNA was used as a control (Qiagen, Venlo, The Netherlands). The cells were transfected with 20 nM siRNA using Lipofectamine 2000 (Invitrogen Corp.; Carlsbad, CA, USA) according to the manufacturer's recommendations.

#### 4.6. Reverse Transcription Polymerase Chain Reaction (PCR)

Total RNA (1  $\mu\text{g}$ ) was used to synthesize cDNA using a ReverTra Ace quantitative PCR (qPCR) RT kit (Toyobo, Osaka, Japan). PCR was performed as specified by the manufacturer. PCR products were electrophoresed on 2% agarose gels and visualized using ethidium bromide. The primer sets are listed in Table 3. Primers were synthesized by Sigma-Genosys (Ishikari, Japan).

#### 4.7. Protein Extraction

To prepare whole-cell lysates, oral SCC cells ( $1 \times 10^7$ ) were washed twice with cold PBS, harvested, and lysed with 0.1% SDS-containing RIPA buffer (Thermo Fisher Scientific, Tokyo, Japan) [34]. Cell fractions were extracted using a Cell Fractionation Kit (Abcam, Cambridge, MA, USA), according to the manufacturer's instructions [35]. Protein assays were performed using a Protein Assay Rapid Kit (Wako Pure Chemical Corporation, Osaka, Japan).

#### 4.8. Immunoblot Analysis

Whole-cell lysates of HSC4 cells were prepared as previously described [34]. Lysates (20  $\mu\text{g}$ ) were separated by immunoblot analysis using 12.5% sodium dodecyl sulfate polyacrylamide gel electrophoresis (SDS-PAGE), followed by electrotransfer onto nitrocellulose filters. The filters were incubated with primary antibodies, followed by secondary peroxidase-conjugated IgG antibodies (Medical and Biological Laboratories). An anti-tubulin antibody was used for loading control

(Oncogene Research Products, Cambridge, MA, USA). The immune complexes were visualized using an Enhanced Chemiluminescence Western-blot detection system (Amersham, Aylesbury, UK). Antibodies against YAP1, phosphorylated YAP1 (pS127), GAPDH (glyceraldehyde-3-phosphate dehydrogenase), large tumor suppressor kinase 1 (LATS1), phosphorylated LATS (pThr1079) (Cell Signaling Technology, Beverly, MA, USA), tubulin (Zymed Laboratories Inc., South San Francisco, CA, USA), and lamin (Proteintech Group Inc., Rosemont, IL, USA) were used as primary antibodies.

**Table 3.** Primer sets for RT-PCR.

Gene Name	Gene Bank ID	Upper/Lower	Primer Sequence
ME1	NM_002395.5	U L	GGATTGCACACCTGATTGTG TCTTCATGTTTCATGGGCAAA
CDH	Z13009.1	U L	TGCCCAGAAAATGAAAAAGG GTGTATGTGGCAATGCGTTC
CLDN4	NM_001305.4	U L	CTCCATGGGGCTACAGGTAA AGCAGCGAGTCGTACACCTT
HIF1 $\alpha$	AF208487.1	U L	GAAAGCGCAAGTCCTCAAAG TGGGTAGGAGATGGAGATGC
MCT1	AY364258.1	U L	TCCTTTTATCCTGCCACACC GCATGCTGTTTTCCTTCTGC
MMP2	KR710613.1	U L	ATGACAGCTGCACCACTGAG ATTTGTTGCCAGGAAAGTG
MMP9	NM_004994.3	U L	TTGACAGCGACAAGAAGTGG GCCATTCACGTCGTCCTTAT
MMP7	NM_002423.5	U L	GAGTGCCAGATGTTGCAGAA AAATGCAGGGGGATCTCTTT
c-Myc	NM_002467.4	U L	TTCGGGTAGTGAAAACCAG CAGCAGCTCGAATTTCTTCC
GAPDH	BC025925.1	U L	GAGTCAACGGATTTGGTCGT TTGATTTTGGAGGGATCTCG

#### 4.9. Mitochondrial Staining

Mitochondria were stained with tetramethyl rhodamine (TMRE) and dihydrorhodamine 123 (DHR) at 37 °C for 24 h to assess mitochondrial membrane voltage (Takara Bio Inc., Kusatsu, Japan) and observed via fluorescence microscopy (Keyence, Osaka, Japan).

#### 4.10. Determination of Concentrations of Lactate and Nuclear YAP

Lactate concentrations were determined using a D-Lactate Assay kit (Cayman Chemical, Ann Arbor, MI, USA). YAP concentrations were determined using a human YAP1 ELISA kit (Abcam). The assays were performed according to the manufacturers' instructions.

#### 4.11. Statistical Analysis

Statistical significance was assessed using the  $\chi^2$ -test and Student's *t*-test with the assumption of Gaussian distribution according to the Kolmogorov and Smirnov method. Linear regression was evaluated with Spearman's *r*. Analyses were performed using InStat software (GraphPad, Los Angeles, CA, USA). Statistical significance was defined as  $p < 0.05$ .

## 5. Conclusions

As shown in the schematic illustration (Figure 6), in cancer cells at the tumor invasive front, a hypoxic environment increases lactate secretion due to switching of the energy metabolism from

oxidative phosphorylation to glycolysis following ME1 overexpression and decreases extracellular pH and YAP activation. These alterations promote tumor budding by enhancing EMT of cancer cells with stem cell properties and invasion ability. Thus, tumor budding is a marker of the malignant phenotype of cancer; it is considered that budding cancer cells themselves have acquired a malignant phenotype. In addition, in our study, the correlation between tumor budding and ME1 expression increased with the progression of cancer, suggesting that ME1 strongly promotes tumor budding and the malignant phenotype in OSCCs. We previously reported the effectiveness of inhibition of ME1 using lantanid [11]; however, this strategy has issues related to lantanid's derivatives and stability. In the future, the discovery of a more useful ME1 inhibitor is desired for targeting tumor budding.

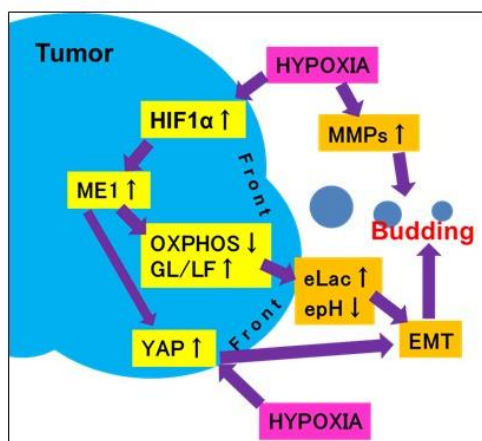


**Figure 6.** Schema of the mechanism of tumor budding. When cancer cells at the invasive front suffer hypoxia, they overexpress ME1, which leads to reprogramming of the energy metabolism from oxidative phosphorylation to glycolysis/lactate fermentation. This subsequently increases lactate secretion and decreases the extracellular pH and YAP activation. Due to these alterations, cancer cells at the invasive front undergo budding via an increase in stemness, invasion ability, and EMT phenotype. epH, extracellular pH; eLac, extracellular lactate; OXPHOS, oxidative phosphorylation; MMP, matrix metalloproteinase.

**Author Contributions:** C.N. carried out most of the experiments and wrote the manuscript; R.F.-T., K.F., Y.L. assisted in the histopathological analysis; I.K., T.M., K.G. assisted in the cellular experiment; S.M., T.S., S.K. assisted in the immunoblotting experiment; H.O. assisted in the statistical analyses; K.Y. assisted in the analysis and interpretation of the results; T.K., H.K. conceived the project and designed the experiments. All authors have read and agreed to the published version of the manuscript.

**Funding:** This work was supported by MEXT KAKENHI Grant Numbers 19K19332 (CN), 18K09539 (KY), 20K21659 (HK), 19K16564 (RFT), 20K18007 (SK).

**Acknowledgments:** The authors thank Tomomi Masutani for expert assistance with the preparation of this manuscript.

**Conflicts of Interest:** The authors have no conflict of interest to declare.

## Abbreviations

EMT	epithelial–mesenchymal transition
HIF	hypoxia-inducible factor
ME	malic enzyme
OSCC	oral squamous cell carcinoma
CLDN	claudin
LDHA	lactate dehydrogenase A
PDH	pyruvate dehydrogenase
DCA	dichloroacetate
GPCR	G protein-coupled receptor

## References

1. Prall, F. Tumour budding in colorectal carcinoma. *Histopathology* **2007**, *50*, 151–162. [[CrossRef](#)] [[PubMed](#)]
2. Li, H.; Xu, F.; Li, S.; Zhong, A.; Meng, X.; Lai, M. The tumor microenvironment: An irreplaceable element of tumor budding and epithelial-mesenchymal transition-mediated cancer metastasis. *Cell Adh. Migr.* **2016**, *10*, 434–446. [[CrossRef](#)] [[PubMed](#)]
3. Kanazawa, H.; Mitomi, H.; Nishiyama, Y.; Kishimoto, I.; Fukui, N.; Nakamura, T.; Watanabe, M. Tumour budding at invasive margins and outcome in colorectal cancer. *Colorectal. Dis.* **2008**, *10*, 41–47. [[CrossRef](#)] [[PubMed](#)]
4. Mitrovic, B.; Schaeffer, D.F.; Riddell, R.H.; Kirsch, R. Tumor budding in colorectal carcinoma: Time to take notice. *Mod. Pathol.* **2012**, *25*, 1315–1325. [[CrossRef](#)]
5. Almangush, A.; Pirinen, M.; Heikkinen, I.; Mäkitie, A.A.; Salo, T.; Leivo, I. Tumour budding in oral squamous cell carcinoma: A meta-analysis. *Br. J. Cancer* **2018**, *118*, 577–586. [[CrossRef](#)]
6. Yamakawa, N.; Kirita, T.; Umeda, M.; Yanamoto, S.; Ota, Y.; Otsuru, M.; Okura, M.; Kurita, H.; Yamada, S.; Hasegawa, T.; et al. Tumor budding and adjacent tissue at the invasive front correlate with delayed neck metastasis in clinical early-stage tongue squamous cell carcinoma. *J. Surg. Oncol.* **2019**, *119*, 370–378. [[CrossRef](#)]
7. Elseragy, A.; Salo, T.; Coletta, R.D.; Kowalski, L.P.; Haglund, C.; Nieminen, P.; Mäkitie, A.A.; Leivo, I.; Almangush, A. A Proposal to Revise the Histopathologic Grading System of Early Oral Tongue Cancer Incorporating Tumor Budding. *Am. J. Surg. Pathol.* **2019**, *43*, 703–709. [[CrossRef](#)]
8. Georges, L.M.; Verset, L.; Zlobec, I.; Demetter, P.; De Wever, O. Impact of the Microenvironment on Tumour Budding in Colorectal Cancer. *Adv. Exp. Med. Biol.* **2018**, *1110*, 101–111.
9. Wong, C.C.; Kai, A.K.; Ng, I.O. The impact of hypoxia in hepatocellular carcinoma metastasis. *Front. Med.* **2014**, *8*, 33–41. [[CrossRef](#)]
10. Al Tameemi, W.; Dale, T.P.; Al-Jumaily, R.M.K.; Forsyth, N.R. Hypoxia-Modified Cancer Cell Metabolism. *Front. Cell Dev. Biol.* **2019**, *7*, 4. [[CrossRef](#)]
11. Nakashima, C.; Yamamoto, K.; Fujiwara-Tani, R.; Luo, Y.; Matsushima, S.; Fujii, K.; Ohmori, H.; Sasahira, T.; Sasaki, T.; Kitadai, Y.; et al. Expression of cytosolic malic enzyme (ME1) is associated with disease progression in human oral squamous cell carcinoma. *Cancer Sci.* **2018**, *109*, 2036–2045. [[CrossRef](#)] [[PubMed](#)]
12. Frenkel, R. Regulation and physiological functions of malic enzymes. *Curr. Top Cell Regul.* **1975**, *9*, 157–181. [[PubMed](#)]
13. Rose, I.A. How fumarase recycles after the malate → fumarate reaction. Insights into the reaction mechanism. *Biochemistry* **1998**, *37*, 17651–17658. [[CrossRef](#)] [[PubMed](#)]
14. Wehrle, J.P.; Ng, C.E.; McGovern, K.A.; Aiken, N.R.; Shungu, D.C.; Chance, E.M.; Glickson, J.D. Metabolism of alternative substrates and the bioenergetic status of EMT6 tumor cell spheroids. *NMR Biomed.* **2000**, *13*, 349–360. [[CrossRef](#)]
15. Liao, R.; Ren, G.; Liu, H.; Chen, X.; Cao, Q.; Wu, X.; Li, J.; Dong, C. ME1 promotes basal-like breast cancer progression and associates with poor prognosis. *Sci. Rep.* **2018**, *8*, 1–10. [[CrossRef](#)]
16. Sobin, L.H.; Gospodarowicz, M.; Wittekind, C. *UICC TNM Classification of Malignant Tumours*, 7th ed.; John Wiley & Sons, Inc.: New York, NY, USA, 2009.
17. Simonetti, O.; Lucarini, G.; Rubini, C.; Goteri, G.; Zizzi, A.; Staibano, S.; Campanati, A.; Ganzetti, G.; Di Primio, R.; Offidani, A. Microvessel density and VEGF, HIF-1 $\alpha$  expression in primary oral melanoma: Correlation with prognosis. *Oral. Dis.* **2013**, *19*, 620–627. [[CrossRef](#)]
18. Nakashima, C.; Yamamoto, K.; Kishi, S.; Sasaki, T.; Ohmori, H.; Fujiwara-Tani, R.; Mori, S.; Kawahara, I.; Nishiguchi, Y.; Mori, T.; et al. Clostridium perfringens enterotoxin induces claudin-4 to activate YAP in oral squamous cell carcinomas. *Oncotarget* **2020**, *11*, 309–321. [[CrossRef](#)]
19. Elvidge, G.P.; Glenny, L.; Appelhoff, R.J.; Ratcliffe, P.J.; Ragoussis, J.; Gleadle, J.M. Concordant regulation of gene expression by hypoxia and 2-oxoglutarate-dependent dioxygenase inhibition: The role of HIF-1 $\alpha$ , HIF-2 $\alpha$ , and other pathways. *J. Biol. Chem.* **2006**, *281*, 15215–15226. [[CrossRef](#)]
20. Li, Y.Y.; Zheng, Y.L. Hypoxia promotes invasion of retinoblastoma cells in vitro by upregulating HIF-1 $\alpha$ /MMP9 signaling pathway. *Eur. Rev. Med. Pharmacol. Sci.* **2017**, *21*, 5361–5369.

21. Liu, H.L.; Liu, D.; Ding, G.R.; Liao, P.F.; Zhang, J.W. Hypoxia-inducible factor-1 $\alpha$  and Wnt/ $\beta$ -catenin signaling pathways promote the invasion of hypoxic gastric cancer cells. *Mol. Med. Rep.* **2015**, *12*, 3365–3373. [[CrossRef](#)]
22. Sullivan, R.; Graham, C.H. Hypoxia-driven selection of the metastatic phenotype. *Cancer Metastasis Rev.* **2007**, *26*, 319–331. [[CrossRef](#)] [[PubMed](#)]
23. Xing, F.; Okuda, H.; Watabe, M.; Kobayashi, A.; Pai, S.K.; Liu, W.; Pandey, P.R.; Fukuda, K.; Hirota, S.; Sugai, T.; et al. Hypoxia-induced Jagged2 promotes breast cancer metastasis and self-renewal of cancer stem-like cells. *Oncogene* **2011**, *30*, 4075–4086. [[CrossRef](#)] [[PubMed](#)]
24. Hockel, M.; Schlenger, K.; Aral, B.; Mitze, M.; Schaffer, U.; Vaupel, P. Association between tumor hypoxia and malignant progression in advanced cancer of the uterine cervix. *Cancer Res.* **1996**, *56*, 4509–4515. [[PubMed](#)]
25. Mezheyeuski, A.; Nerovnya, A.; Bich, T.; Tur, G.; Ostman, A.; Portyanko, A. Inter- and intra-tumoral relationships between vasculature characteristics, GLUT1 and budding in colorectal carcinoma. *Histol. Histopathol.* **2015**, *30*, 1203–1211. [[PubMed](#)]
26. Dong, C.; Yuan, T.; Wu, Y.; Wang, Y.; Fan, T.W.; Miriyala, S.; Lin, Y.; Yao, J.; Shi, J.; Kang, T.; et al. Loss of FBP1 by Snail-mediated repression provides metabolic advantages in basal-like breast cancer. *Cancer Cell* **2013**, *23*, 316–331. [[CrossRef](#)]
27. Justus, C.R.; Dong, L.; Yang, L.V. Acidic tumor microenvironment and pH-sensing G protein-coupled receptors. *Front. Physiol.* **2013**, *4*, 354. [[CrossRef](#)]
28. Luo, Y.; Kishi, S.; Sasaki, T.; Ohmori, H.; Fujiwara-Tani, R.; Mori, S.; Goto, K.; Nishiguchi, Y.; Mori, T.; Kawahara, I.; et al. Targeting claudin-4 enhances chemosensitivity in breast cancer. *Cancer Sci.* **2020**, *111*, 1840–1850. [[CrossRef](#)]
29. McDonald, P.C.; Chafe, S.C.; Dedhar, S. Overcoming Hypoxia-Mediated Tumor Progression: Combinatorial Approaches Targeting pH Regulation, Angiogenesis and Immune Dysfunction. *Front. Cell Dev. Biol.* **2016**, *4*, 27. [[CrossRef](#)]
30. Greenhough, A.; Bagley, C.; Heesom, K.J.; Gurevich, D.B.; Gay, D.; Bond, M.; Collard, T.J.; Paraskeva, C.; Martin, P.; Sansom, O.J.; et al. Cancer cell adaptation to hypoxia involves a HIF-GPRC5A-YAP axis. *EMBO Mol. Med.* **2018**, *10*. [[CrossRef](#)]
31. Zhang, X.; Li, Y.; Ma, Y.; Yang, L.; Wang, T.; Meng, X.; Zong, Z.; Sun, X.; Hua, X.; Li, H. Yes-associated protein (YAP) binds to HIF-1 $\alpha$  and sustains HIF-1 $\alpha$  protein stability to promote hepatocellular carcinoma cell glycolysis under hypoxic stress. *J. Exp. Clin. Cancer Res.* **2018**, *37*, 216. [[CrossRef](#)]
32. Bhattacharya, D.; Azambuja, A.P.; Simoes-Costa, M. Metabolic Reprogramming Promotes Neural Crest Migration via Yap/Tead Signaling. *Dev. Cell* **2020**, *53*, 199–211.e6. [[CrossRef](#)] [[PubMed](#)]
33. Kuniyasu, H.; Yano, S.; Sasaki, T.; Sasahira, T.; Sone, S.; Ohmori, H. Colon cancer cell-derived high mobility group 1/amphoterin induces growth inhibition and apoptosis in macrophages. *Am. J. Pathol.* **2005**, *166*, 751–760. [[CrossRef](#)]
34. Kuniyasu, H.; Oue, N.; Wakikawa, A.; Shigeishi, H.; Matsutani, N.; Kuraoka, K.; Ito, R.; Yokozaki, H.; Yasui, W. Expression of receptors for advanced glycation end-products (RAGE) is closely associated with the invasive and metastatic activity of gastric cancer. *J. Pathol.* **2002**, *196*, 163–170. [[CrossRef](#)] [[PubMed](#)]
35. Matsushima-Otsuka, S.; Fujiwara-Tani, R.; Sasaki, T.; Ohmori, H.; Nakashima, C.; Kishi, S.; Nishiguchi, Y.; Fujii, K.; Luo, Y.; Kuniyasu, H. Significance of intranuclear angiotensin-II type 2 receptor in oral squamous cell carcinoma. *Oncotarget* **2018**, *9*, 36561–36574. [[CrossRef](#)] [[PubMed](#)]

